

INTEGRAL FLUIDIC GENERATOR OF MICROBUBBLES

Václav Tesař, Miroslav Jílek

Institute of Thermomechanics v.v.i., Academy of Sciences of the Czech Republic, Prague

Abstract: Very small gas bubbles dispersed in liquid are desirable in many applications. If smaller than 1 mm in diameter, they are called *microbubbles* and differ from large bubbles not only quantitatively but even in several qualitative properties. Until recently, the advantages they offer have been little used because of generally low efficiency of microbubble generation methods. A solution was found in pulsating the gas flow into the submerged aerator by a fluidic oscillator. At present, the oscillator and aerator are separate devices. The flow pulsation is strongly damped in the connecting tubes. New solution presented in this paper relies on oscillator robustness and no need for maintenance, which allows integrating it with the aerator into a single body submerged in the liquid. Small bubble size requires driving frequency much higher than has been so far applied. The present paper shows some of the ways leading to high frequencies – in particular the use of dominant third harmonic of the basic switching frequency.

1. Introduction

Gas dispersed in a liquid in the form of small bubbles is an everyday experience – everybody has seen them, e.g. in carbonated beverages [1, 2], where they are released by decreased gas solubility after a decrease in pressure (Henry's law). However, the two-phase medium of gas bubbles in liquid is of high importance for many industrial and biomedical engineering processes. Bringing the gas into the liquid is most commonly done by percolating it through many small exits from a submerged aerator body. The diffusion transport across the gas/liquid interface is the more effective the smaller the bubbles are – so that preferred are microbubbles [3], defined as being of diameter smaller than 1 mm. There is a quite widespread belief that small bubbles are automatically obtained if the aerator exits are of small size. This is not always true, because of the phenomenon known as instability of parallel bubble formation [4]. It is

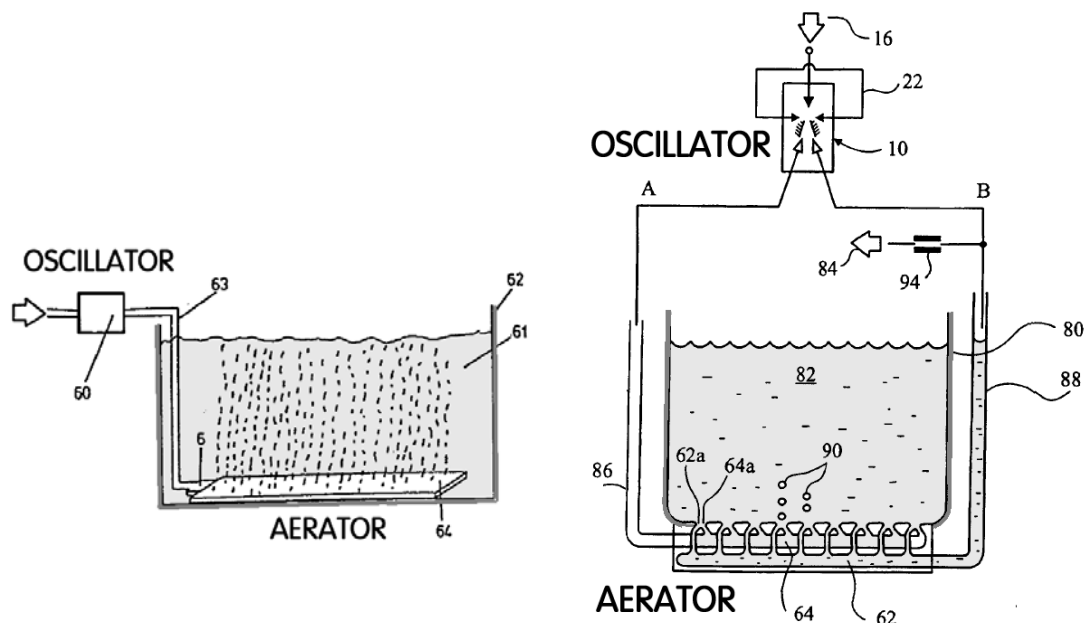


Fig. 1 (Left) Drawing adapted from ref. [5]: a typical configuration of microbubble generator with the usual placement of the oscillator 60 outside the water-processing vessel. Of course, oscillation is inevitably severely damped in the supply line 63 carrying it into the aerator body 64.

Fig. 2 (Right) Drawing by a professional draughtsman from the European Patent [6, 7]: the first author's design of a microbubble generator with fluidic diverter type oscillator, the latter again well separated from the aerator.

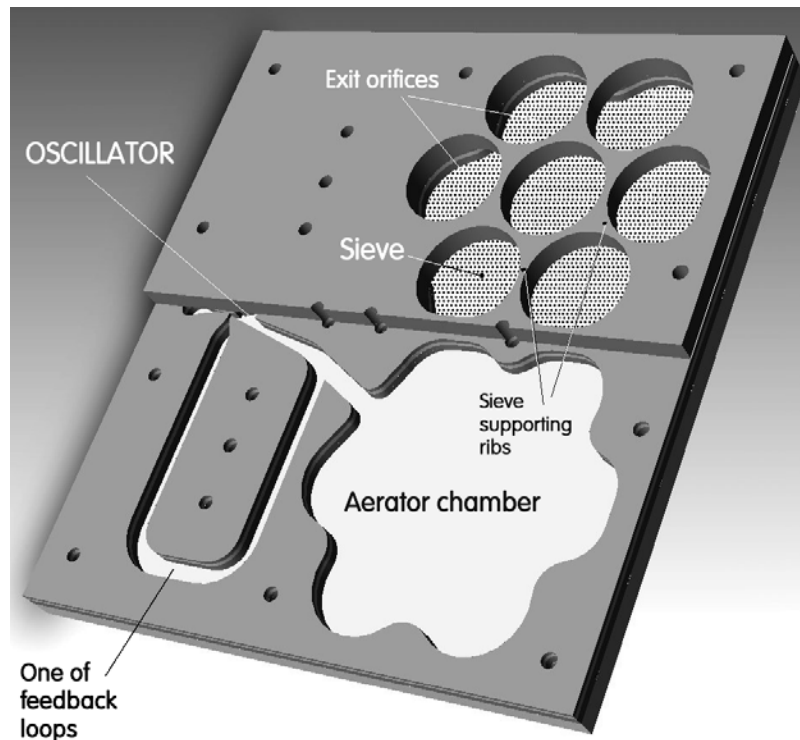


Fig. 3 The integral generator as designed by the first author (V.T.). One half of the top cover plate is shown removed to display the internal cavities, made by laser cutting in stainless steel plates. In the final operational version the plates will be welded together; in the present laboratory version they are held by screws passing through the holes visible in the picture.

difficult to avoid, being a direct consequence of the fundamental Laplace-Young law (an inverse proportionality between pressure difference across the bubble surface and the surface curvature radius). Once one bubble - among those generated in parallel exits - becomes larger, its lower internal pressure attracts the gas from other exits, usually making them inoperative. Instead of the expected many small bubbles one obtains a single large bubble (or a few of them). Methods how to generate microbubbles without this effect (using e.g. ultrasound) are known, but generally are not energetically efficient. Thus the potential advantages offered by microbubbles could not be so far utilised. Only recently an energy-efficient method was discovered [6, 7], based on oscillation of the gas supply flow into the aerator - Figs. 1, 2. This has opened a way to use of microbubbles in many promising industrial processes. The key factor is generating the flow pulsation by means of fluidic no-moving-part oscillators. Apart from their good efficiency, fluidic oscillators offer the advantage of operating without motion or deformation of mechanical components. This ensures maintenance-free operation, long life, and high reliability. Also, the absence of inertia of moving mechanical components makes, in principle, possible to achieve quite high oscillation frequencies.

There are several known principles of fluidic oscillators [8]. Nevertheless their most common layout (others being used very rarely) is based on hydrodynamic instability of jet flows caused by a negative jet-deflection feedback. Usually the basic component is a fluidic amplifier – a device in which the large output flow rate is controlled by a weak input flow. The negative feedback generating the instability and self-excited oscillation is set up by arranging a flowpath (usually by a connecting channel or tube) that takes a small part of the output flow back into the control terminal. Commonly used amplifiers in fluidic oscillators are of the jet-deflection, bistable diverting type, with the bistability obtained by the Coanda effect. This is attachment of the jet alternatively to one of a pair of attachment walls positioned near the main jet flow path. The walls lead the jet flow into each into one from a pair of exit terminals — from where the feedback channels return the fluid back into the control inlet on the same side (a layout patented by Warren in 1962). Because of the instability, the jet cannot stay straight and must attach to one of the attachment walls – where, however, the feedback action prevents it from remaining and forces it to switch to the opposite side, where later the same effect takes place.

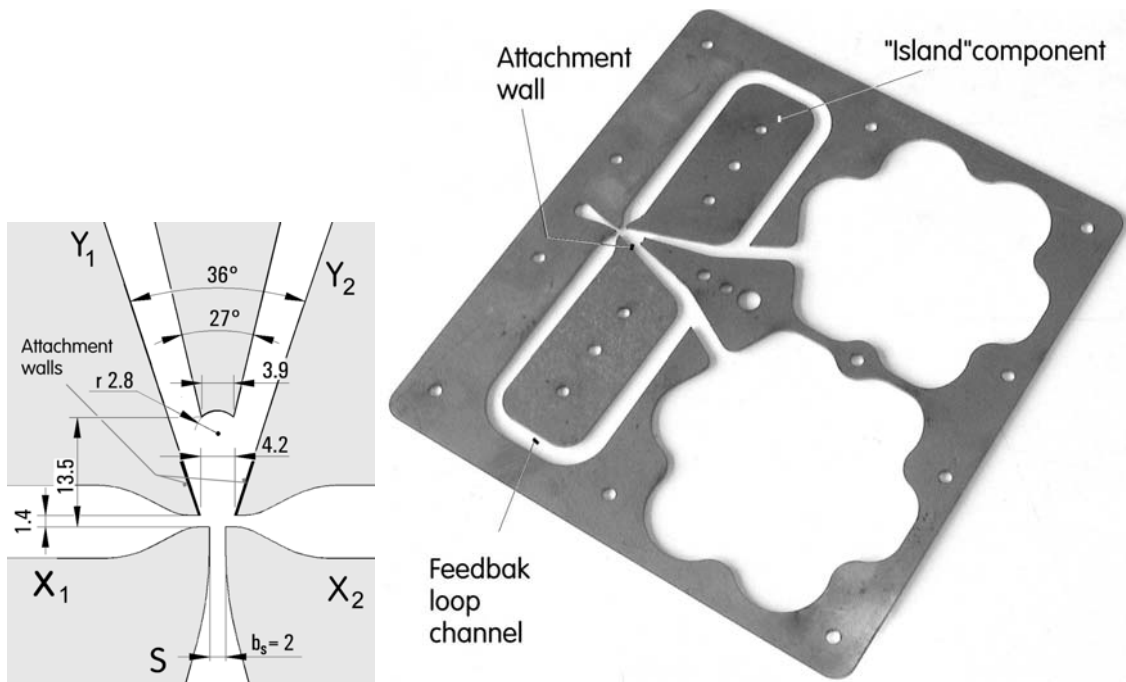


Fig. 4 (Left) The core part of the diverter amplifier as it was used in the initial design of the integral unit. The geometry was scaled from the oscillator discussed in ref. [9], historically related to an early successful amplifier design described in [10]. In later stages of development the attachment walls were removed.

Fig. 5 (Right) Photograph of the main plate. The amplifier according to Fig. 4 is converted into the oscillator by addition of the two feedback loop channels. Cavities closed on top and below by cover plates (as seen in Fig. 5). Positioning of the "island" components complicated the manufacture and they were later removed, which incidentally increased the oscillation frequency.

In spite of their simplicity the fluidic oscillators recently introduced for the task of microbubble generation are mostly seen as a new concept and often viewed with certain apprehension (after all, it is true that designing an efficient oscillator is by no means a simple task, sometimes compared to "black magic"). Thus while the microbubble producing aerators are necessarily submerged, usually positioned at the bottom of the vessel into which the air is percolated, the oscillators are usually at a location high above, where there is a free access to them for expected interventions. This is typically shown in the illustrations in Figs. 1 and 2. This separation of the two essential parts necessitates providing rather long connecting tubes leading from the oscillator exits into the aerator. Unfortunately, the oscillator-generated oscillation tend to be strongly damped in these tubes.

2. New integral design

The first author (V. T.) found a solution to this problem of pulsation damping - and to several associated problems - in a unit in which the oscillator is integrated with the aerator so that they form a single submerged body. There are no connecting tubes. The resultant unit also becomes less prone to damage. In several envisaged applications - such as, e.g., in waste water processing - the generator has to operate in a quite adverse environment, where accidental damage to the tubes cannot be excluded. It is certainly an advantage of the integrated unit that it is compact and may be wholly made from a mechanically resistant material, without the soft interconnecting tubes as they are currently used (and without the vulnerable tube connections, which are currently fixed during the assembly of the system on the site - an expensive activity). In their manufacturing in the integral unit, both oscillator and aerator are made simultaneously in the same manufacturing operation, which also makes the whole system less expensive. Probably most important among the advantages of the integration is the fact that the collaboration of the two devices provides an obvious opportunity for their mutual matching. Because of non-linearity typical for fluidics, matching of fluidic device properties - similar to the approach discussed

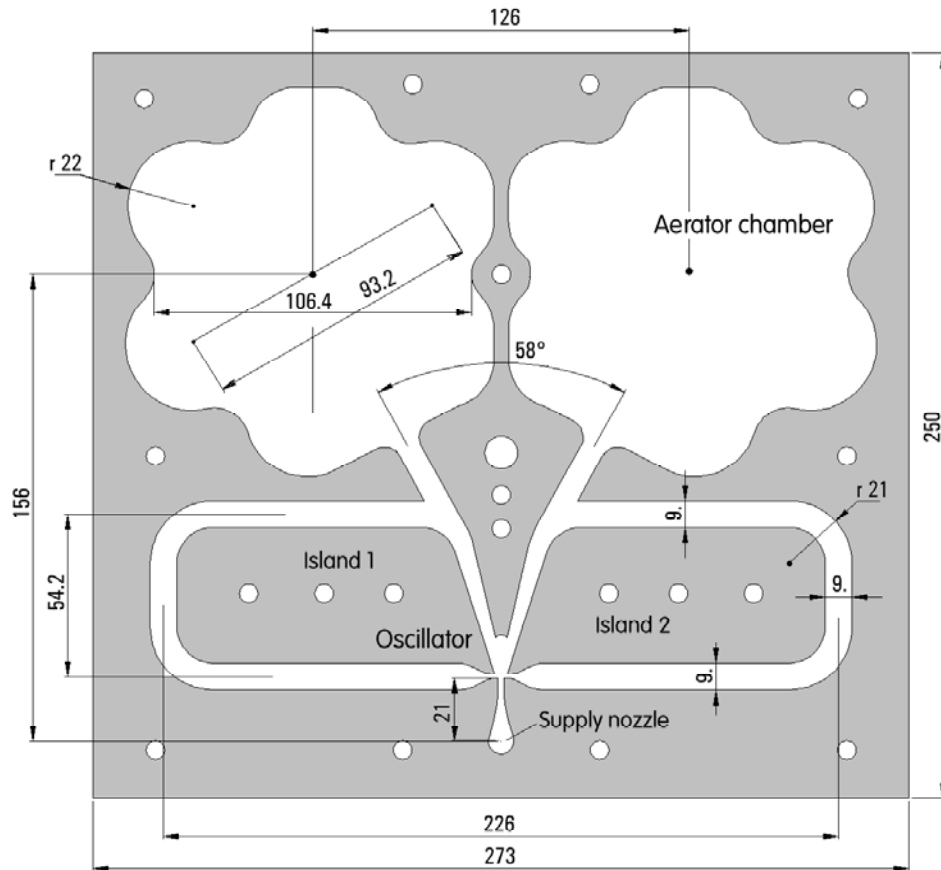


Fig. 6 Workshop drawing of the main plates with the working cavities made by laser cutting – as designed in the initial version. Changes made later are discussed in the text. .

in [11, 12] - is generally a problem far from easy to tackle. That it is not to be taken easily is seen from the experience of other researchers that have demonstrated generation of microbubbles, e.g., in [13, 14]. They have typically discovered that the oscillator requests a relatively large supplied air flow rate (mainly because the Coanda effect of the jet attachment ceases to be effective at low Reynolds numbers) while the relatively small aerators so far used can handle only small air flow rates. Because most experimental investigations so far were aimed at mere demonstrations of microbubble generation, the problem was solved by releasing a considerable part of the pulsatile flow from the oscillator into atmosphere. This may be acceptable in laboratory tests but economically untenable for an industrial scale process. In the integrated unit discussed here, the matching is seen in Figs. 3 and 5 already from the oscillator of rather small dominant air flow cross section — which is the cross section of the supply nozzle exit, only $b_S = 2$ mm wide — integrated with the large available exit areas provided by the 14 large aerator-exit holes (of approximately 44 mm diameter each, Fig. 8) – of course, the bubble generating exits are the distributed throughout these holes as the free spaces in a woven metal textile. It should be noted that from the matching point of view there are in this unit (Figs. 3, 5) actually two mutually independent aerators, each supplied alternatively from one of the two exit terminals of the diverter-type oscillator.

The unit used in the tests the results of which are discussed below was made as a stack of rectangular stainless steel plates; the size of the rectangle was 273 mm x 250 mm. The oscillator cavities were made by laser cutting in three identical thin plates, of 2 mm thickness, shaped according to Fig. 6. By varying the number of these plates (one, two, or three in the stack) it was possible to vary the aspect ratio (depth to nozzle width). The cavities were closed from above as well as from below by thicker, 8 mm, top and bottom cover plates, respectively.

The feedback action was secured by means of the two symmetrically placed feedback channels, 9 mm wide, as shown in Fig. 5. Earlier first author's oscillator designs, for example the one discussed in

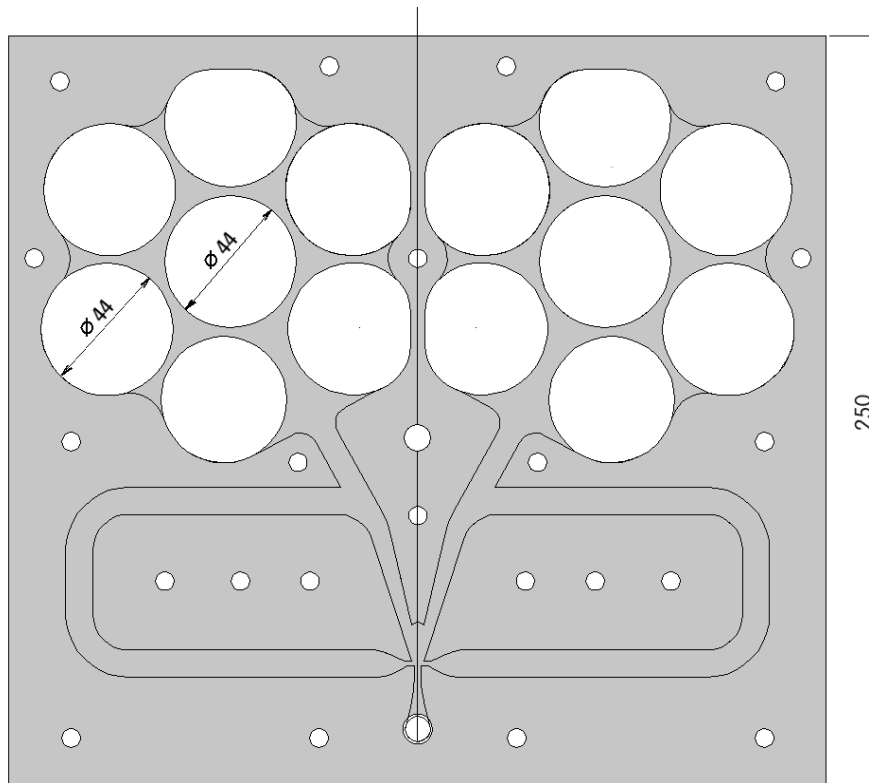


Fig. 7 Drawing of the top cover plate with the 14 large aerator-exit holes (into which the generated microbubbles enter from the metal textile sieve supported by the ribs left between these 44 mm holes. In principle, there are actually two aerators, each with the simultaneously activated 7 holes on one side of the symmetry axis.

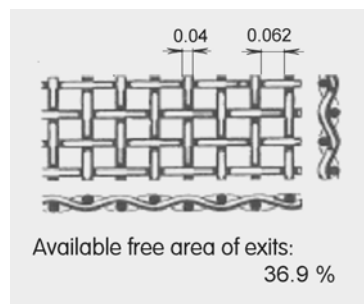


Fig. 8 Enlarged view of the stainless steel woven textile sieve, which is in the integral unit clamped under the top cover plate.

[9], preferred – because of simplicity - the single-loop feedback attributed to Spyropoulos [8]. Recent experience, however, has shown that the pressure difference that drives the feedback flow in this configuration is usually smaller, leading to the rather high lower limit of Reynolds numbers below which the oscillator ceases to oscillate. The Warren's layout with the two loops, finally selected for the integral unit, makes the oscillation more reliable and kept running at smaller flow rates. Problems with the matching to the properties of the aerators were likely to lead to a low limit being a quite important factor.

The layout of the integral unit as a stack of plates made not possible to arrange the feedback loops in the form usually reported, i.e. made from a length of tubing (such as Tygon tubes) connected to terminal ferrules (which makes oscillation frequency easily adjustable by cutting the tubes to various lengths). Whatever chosen configuration of the loops, in the integral unit necessitated them to be positioned inside the main plates of the stack, in the form of channels cut in the plate (simultaneously with cutting the amplifier cavities). An inevitable unpleasantness arose with the "islands" (Fig. 6) – those parts of the original plate on the inner side of the loops, which during the laser cutting became

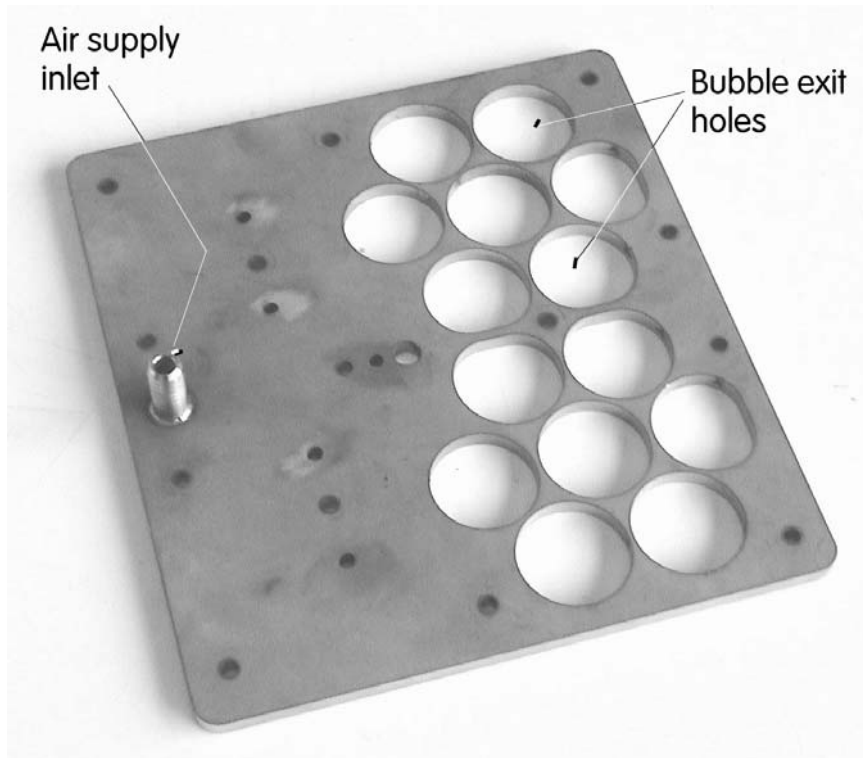


Fig. 9 Photograph of the top cover plate. Note the presence of the air supply inlet at left, leading the compressed air into the supply nozzle of the oscillator (cf. Fig. 6). Through the large exit holes pass the microbubbles generated by air percolation through the sieve (Fig. 8) which is clamped under this top plate.

unsupported and fell out. The unpleasant factor is the resultant complicated manufacturing of the unit since it is necessary to put these “islands” back into the plate and secure there their exact positions. This positioning was done by precisely drilled holes in the “islands” and corresponding positioning dowels, fixed in the bottom and top cover plate (two dowels per each “island” are seen e.g. in Figs. 3, 5, 6, and 7). This positioning are a manual — and hence expensive — manufacturing step.

The actual aerator exits orifices, by percolation through which the microbubbles are formed, are the free areas between fine stainless-steel wires of a woven metal textile, as shown in Fig. 7. This metal fabric, in the shape of the same 273 mm x 250 mm rectangle as the plates in the stack, was clamped under the top cover plate with the large exit holes — the photograph of which is presented in Fig. 9. The

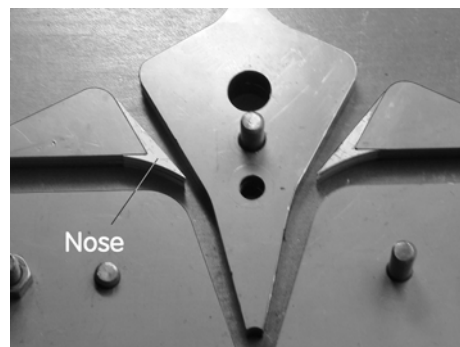
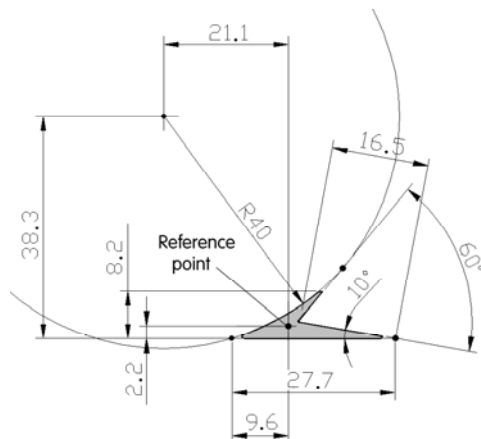


Fig. 10 (Left) Part of the workshop drawing of the sharp-edged “noses” that were added to the inlets into the feedback channels. They force into these channels more air from the flow on the active side.

Fig. 11 (Right) Detail photograph of the feedback channel inlets with the added “noses”.

material of the wires was steel grade 14 404, the wire diameter was 0.04 mm and the width of the available exit openings was 0.062 mm. This metal fabric is rather delicate and so as to prevent its being stressed excessively it is supported from above by the ribs that are left between the large 44 mm dia holes.

Initial feasibility tests proved a highly disappointing fact: the oscillator did not start oscillating, irrespective of the supplied air flow rate. Typical causes of such problems with the Coanda-effect type of oscillators are too large manufacturing tolerances, resultant in lack of symmetry. The jet then attaches to one attachment wall so strongly that it refuses to be switched to the other side. Investigations of the reason for this failure were hampered by the inaccessibility of the cavities. The metal textile sieve was removed to gain an access to the oscillator exits into aerator chamber and it was found, by load switching the amplifier, that it exhibits a correct the bistable behaviour. The jet, however, remained in the switched states. Obviously, the control flows into the control nozzles that were expected to deflect the jet back from an active side were not sufficiently intensive.

The remedy – which, after an implementation, proved the correctness of this reasoning – was increase of the flow into the feedback loop channel on the active side by sharp-edged “noses” placed at the entrance into the feedback. They deflect into the feedback loop a higher proportion of the air flow. The geometry of the “nose” is presented in Fig. 10 and the photograph of the entrances into the feedback channels with the “noses” in position is in Fig. 11. The next Fig. 12 thus shows the integral oscillator/aerator design with which were obtained the initial oscillator tests.

3. The “island”- less layout with feedback cavities

The most important part of the tests with the initial configuration shown in Fig. 12, were concerned with the frequency of generated oscillation — and its dependence on the supplies air mass flow rate. The importance of these factors was underlined by results of another line of investigations, reported in [15]. It indicated desirability of extremely high frequency of the oscillation for producing small microbubbles. While many early tests with the fluidic oscillators for microbubble generation were made at frequencies typically near to 100 Hz, the conclusions of [15] indicated that natural frequencies of microbubble shape oscillations are at least an order of magnitude higher, at and above 1 kHz. Of course, for effectiveness of the energy transfer to an oscillating object, the driving action has to be applied in resonance, i.e. at the natural frequency.

The “shape oscillation” character is an important factor in the process. The name implies indicates an oscillation during which the volume of the bubble does not vary. What is varied are the deviations of bubble shape from the basic spherical geometry. There is also another, perhaps better known kind of oscillation in which it is the volume that varies while the bubble retains its spherical geometry. This was historically investigated, especially in association with cavitation phenomena, much earlier – already by lord Rayleigh in 1917. After all, the equations that govern this second kind of oscillation are easier to solve since the only variable is the scalar – bubble radius – so that the equation is an ordinary differential equation. The shape oscillation is much more difficult to describe mathematically. Characteristic property of the volume oscillation is the necessity of much higher acting pressure levels. This is the reason why they are out of question in the present context.

Until recently, the character of the dependence of the generated oscillation frequency on the supplied flow rate of the working fluid was known to be of one from two possibilities. Usually, oscillation in fluids without an action of movable mechanical components is characterised by constancy of Strouhal number. As a result, the oscillation frequency is more or less proportional to the supplied flow rate. This is the behaviour found over most of the flow rate range e.g. in the oscillator discussed in [9] – although there were exceptional regimes with locking-in to a resonant conditions of some kind. Much more recent is the other oscillator type, discussed in [16]. In this the frequency is dependent on the length of a resonator channel – and not dependent on the flow rate at all. Very recently, a third, rather strange oscillator version was described in [17]. The oscillation frequency there increased with the flow rate, but the dependence was not the simple proportionality and the fitted straight lines intercepted the vertical axis at a quite high value.. Somewhat surprisingly, the first tests with the discussed integral unit exhibited the very same character of the behaviour as was the case in [17].

While this is a peculiarity, it does not influence the applicability of the oscillator for the intended use in microbubble generation (in fact, the increase at a much slower rate than with the constant Strouhal number may be considered an advantage since it puts less demand on the loading characteristics of the

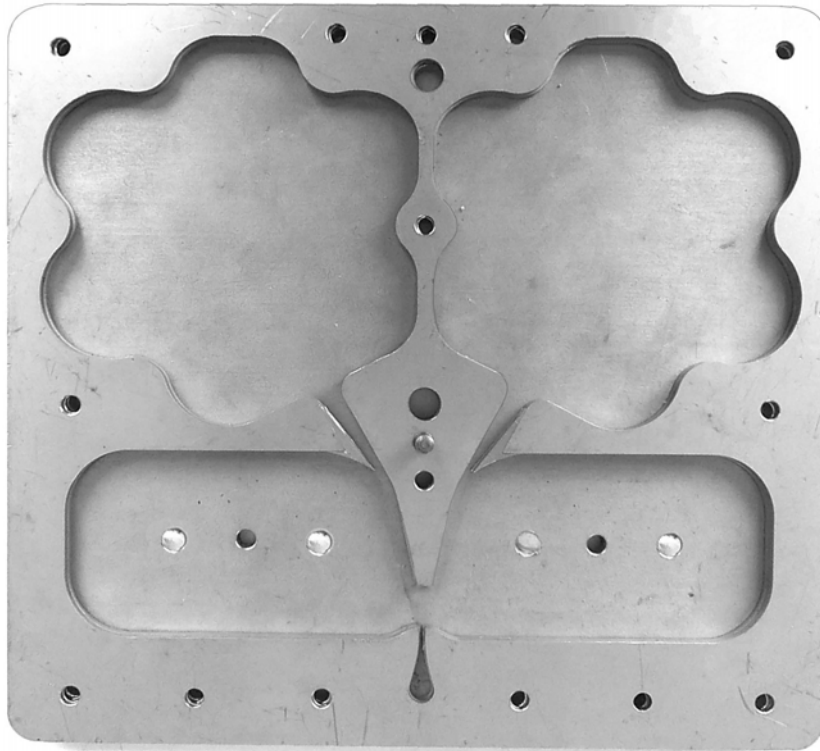


Fig. 12 Photograph of internal cavities of the integrated oscillator/aerator as used in the initial investigations of the oscillator without the “island” components.. Note the sharp-edged noses (cf. Fig. 10) positioned at the entrances into the feedback loop chambers.

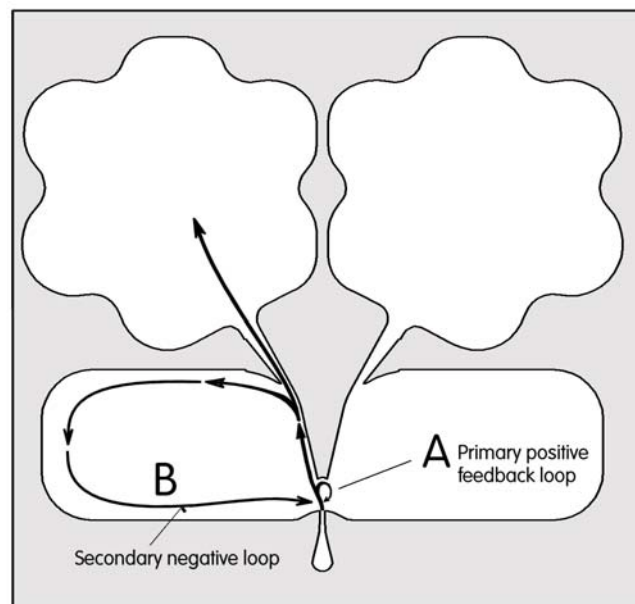


Fig. 13 The first author’s idea of the character of air flow in the cavities. Initially, the positive feedback A keeps the jet deflected despite the absence of the attachment walls. Later the substantial part of the air flow deflected by the “nose”, after having run along the walls of the feedback cavity, forms the vortical loop B that causes the amplifier to switch to the mirror-image position.

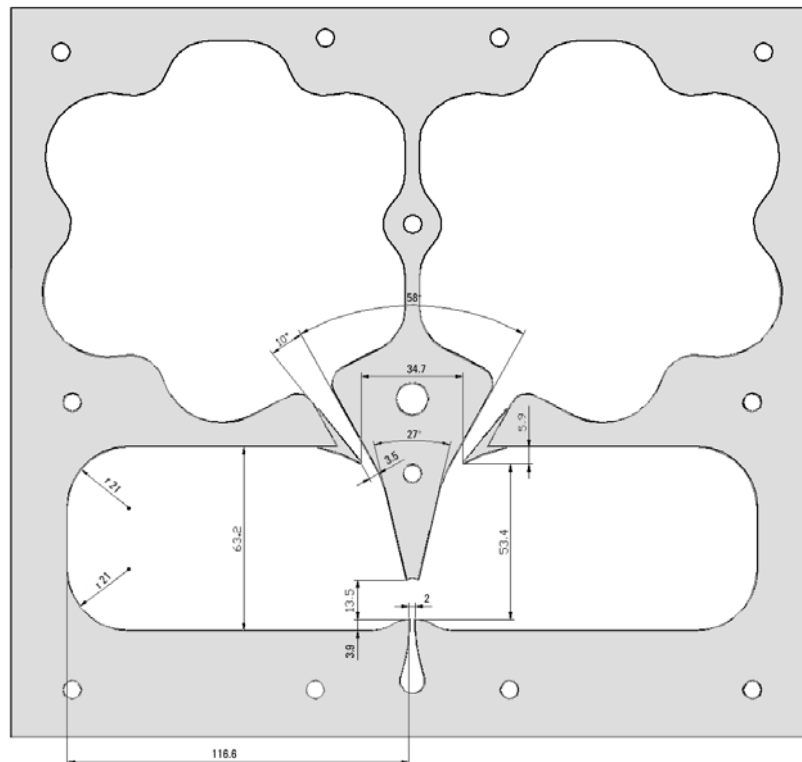


Fig. 14 Basic geometric data of the oscillator when used in the high-frequency experiments.

compressed air supply). What, however, was not welcome, was the level of the generated frequency, which remained in line with oscillators tested earlier. The frequency was found too low.

Another cause of unpleasantness that became evident in the course of the performed tests, were the complications associated with the “islands” (Fig. 6) inside the feedback channel loops (that fell out during the plate manufacture). The aspects of device manufacturing came into foreground.

A test in which the authors did not expect any particular success were series of runs made with the unit assembled as shown in Figs. 12 and 14 - without the “islands”. To a general pleasant surprise, this configuration behave admirably. Not only the oscillator did work. It was discovered that the frequency of the oscillation in this configuration was higher.

Apparently, the cavities that resulted from the removal of the “islands” inside the feedback loop channels made possible air flows of vortical character, as suggested in Fig. 13, which provided the negative feedback action necessary for the oscillation. This is far from obvious. Considering the typically slow start-up and slowing down of vortices, the capability of transferring the feedback signal within the very short available time of an oscillation half-period is surprising.

Not less surprising is the maintained bistability property – which should disappear with the absence of the Coanda effect attachment that acted in the original configuration. Some mechanism keeping the jet bistably deflected obviously must exist in the geometry shown in Fig. 14 — at least during the initial part of each half-period because otherwise the feedback vortex B (Fig. 13) would not have a sufficient opportunity for its motion past the inner wall surface of the cavity. It would not be able to reach the control location at the nozzle exit where it can cause the jet to switch. A plausible explanation for this positive (i.e. deflection retaining) feedback is seen in the action of another, smaller vortical feedback loop. It is the loop A as indicated in Fig. 13. Also this air flow obviously must have a vortical character (i.e. it is not a signal transfer through a channel). The rotating vortex seems to be caused by the bi-cuspid shape of the splitter in its tip opposite to the nozzle exit (Fig. 14). Again, it must be able to change its rotation sense within the oscillation half-period. This bi-cuspid shape has been used by the first author in his previous amplifier designs, being a remnant from the very early configuration discussed in reference [10], in which alternative splitter tip shapes were also tested but found worse.

4. Quest for high frequency – and the third harmonic

As was already said above, a typical feature of early feasibility studies and demonstrations of microbubble generation with fluidic oscillator were made at driving frequencies that were too low from the present point of view. It is obvious that effective excitation must be applied in resonant conditions, with the driving frequency equal to the natural frequency of microbubble shape oscillation. Unfortunately, this natural frequency was not known – a search in existing literature did not provide relevant information. For example, the first author made his early investigations with an oscillator frequency 90 Hz. Later literature reported improvements at higher frequencies – nevertheless the magnitude 267 Hz given very recently in [19] seems to be the upper extreme. After all, very high frequencies are not easy to reach with fluidic oscillators, despite the absence of inertia of moving mechanical components. For example, ref. [16] discusses the problems that were associated in attempts to obtain with the Spyropoulos-Warren configuration palm-sized oscillator a frequency around 300 Hz. Recent investigations of the natural frequency of microbubbles, reported in ref. [18], have shown the natural frequencies being much higher than these values: at least at and preferably above 1 kHz. This is evident from the diagram in Fig. 15, based on results of the investigations described in [18].

A way leading to high generated frequency is available and known – but inconvenient and uneconomical. It is a significant decrease of the oscillator size. High frequency oscillation means short acoustic wavelengths – and this means operation with the resonant channels of short lengths [18]. Correspondingly small must be then the size of the oscillator. Small oscillator is acceptable in laboratory tests – but highly impractical for an industrial process handling the total air flow rate at the industrial scale. Also, the small size means inevitably small generated acoustic power – so that to get the total necessary power levels for a large-scale process would necessitate operating simultaneously a huge number of tiny devices.

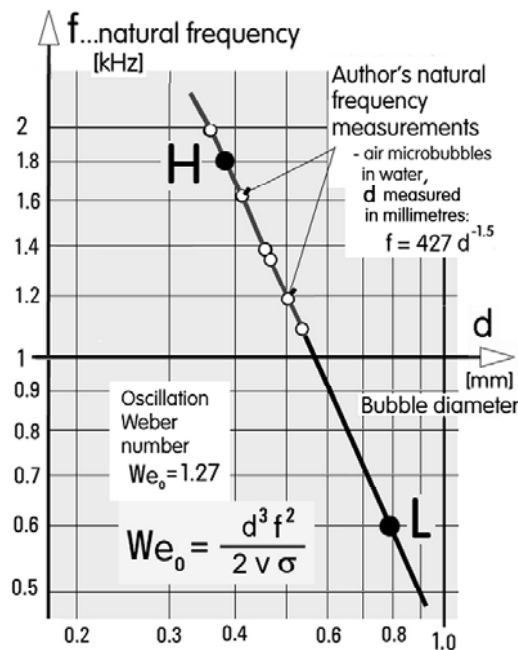


Fig. 15 Natural frequency of microbubble shape oscillation and its dependence on the bubble diameter, as found in the recent investigations [18]. The steep slope of the fitted line leads to unexpectedly high natural frequency - in the kilohertz range - if the microbubbles are to be small. This is because at the small size the microbubbles resist to shape changes by quite high surface tension forces.

In principle it would be possible to design the oscillator in the integral units smaller than the size that was actually used. One of the reasons why it was decided to have it of the $b_S = 2$ mm size was the aspect of manufacturing tolerances. Smaller oscillators may suffer from a relatively poor manufacturing accuracy (because the tolerances are of constant absolute size, usually stated by manufacturers to be ± 0).

1 mm, but in practice found larger). Smaller size oscillators were made and did work. After all, the predecessor of the integral-unit oscillator, described in ref. [9], was smaller, having its supply nozzle width only $b_s = 1.4$ mm. The present larger size $b_s = 2$ mm was chosen mainly for getting the oscillation power level acceptable for practical industrial applications.

As a result of these considerations, the development task of the oscillator in the integral units was formulated as follows: **achieving with the relatively larger 2 mm size the capability to generate frequencies at least 1 kHz.**

The solution was found by accident in the experiments. They indicated that the oscillator with the rounded-rectangular feedback cavities, as shown in Figs. 12 and 14, can oscillate in a regime with dominant third harmonic frequency, i.e. frequency three times higher than the basic frequency of jet switching motions of the jet past the splitter. This fact is demonstrated in the measured frequency dependence on the supplied air mass flow, presented in Fig. 16. The data plotted there were obtained with **three** main (2 mm thick) plates in the stack, i.e. with the resultant depth h of the cavities (the dimension perpendicular to the plane of paper in Fig. 12) equal to $h = 6$ mm.

If the air flow into the oscillator is gradually increased, there is initially a region of too small Reynolds number, at which there is no oscillation. In the oscillators with the Coanda-effect attachment this absence of oscillatory motions in this regime is usually explained as failure of the attachment effect. This effect is based on the pressure differences between the two sides of the jet caused by entrainment of outer air – and at too low Reynolds numbers the entrainment of laminar character is insufficient. It needs turbulent eddies carried with the jet to entrain efficiently the outer air. In the present case, with the attachment walls absent, the exact reason for the absence of oscillation has as yet to be explained – apart from the general fact that at small Reynolds numbers there is relatively more powerful viscous damping.

As the air flow rate is further increased, the oscillator starts oscillating – at a frequency around 500 Hz, which is a quite high value considering the performance of other known oscillators. The frequency initially rises quite rapidly to a value above 550 Hz, but this rapid increase happens over only a small segment of air flows. Very soon thereafter the frequency rises at a much smaller slope. The fitted straight line represents this part of the dependence rather accurately.

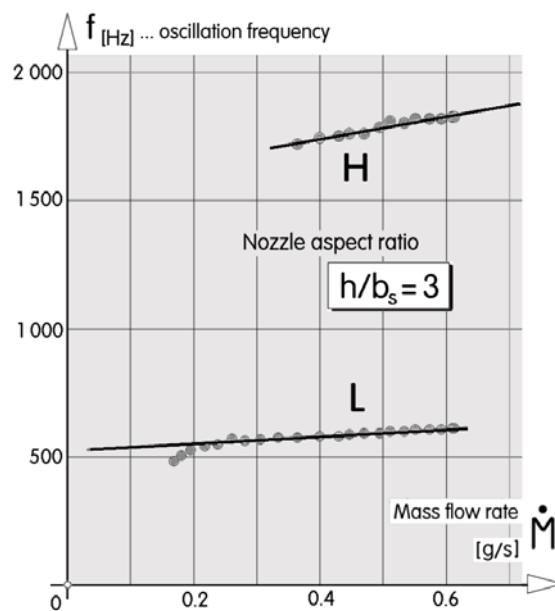


Fig. 16 Results of measurements: dependence of oscillation frequency on the supplied air flow rate in the layout shown in Figs. 12, 13, and 14. Apart from the basic jet-switching frequency f_L , at higher flow rates there is a spectral component with higher frequency f_H , the intensity of which increases with flow rate until it becomes dominant.

In these discussed experiments with gradually increasing supply air flow rate, the oscillation frequency was measured acoustically - by a microphone placed near the exits from the integral unit. The microphone was connected to a signal acquisition card in a computer in which the acoustic signal was analysed by the fast Fourier transform procedure. The air flow was inevitably turbulent (a condition for existence of the Coanda effect), so that the spectral analysis has shown a considerable chaotic component.

High above this noise in the spectrum was a thin sharp peak of organised motions. Its narrow frequency range is, of course, indicative of periodic character. Initially, this peak represented the sideways switching of the jet past the splitter edge, at the frequencies slightly above 500 Hz, increasing with the growing flow rate.

An important phenomenon then occurred when the gradually increased air flow rate reached the magnitude near to 0.35 g/s. From the turbulent noise in the spectrum started rising gradually also another narrow sharp peak. A photograph of the spectrum at this stage (re-arranged into a diagram), is

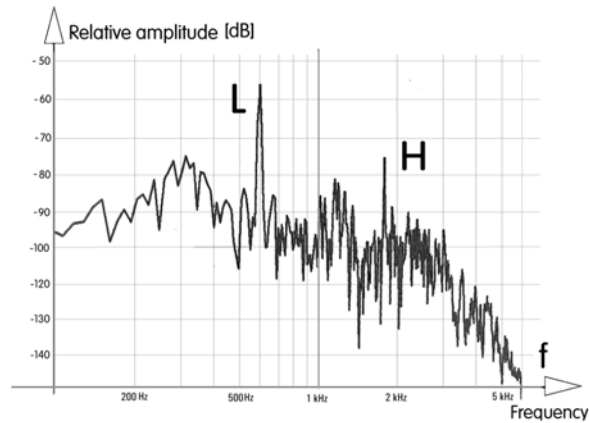


Fig. 17 Spectrum of the acoustic signal obtained by microphone at the oscillator output — obtained in the configuration from Figs. 12 to 14 at the supply air flow rate 0.53 g/s. Immediately apparent are the two high peaks of organised motions: at the basic frequency $f_L = 600$ Hz and its third harmonic $f_H = 1800$ Hz.

seen in Fig. 17. Apart from the basic switching frequency, which at this flow rate already increased to $f_L = 600$ Hz, there is another peak of organised motion, at $f_H = 1800$ Hz. The ratio of the two frequencies f_H and f_L measured at different air flow rates is presented in Fig. 18. From this there is no doubt that the frequency f_H is the third harmonic of the basic jet switching f_L . The third harmonic is found to increase with further increasing flow rate.. At higher flow rates than what is shown in Figs. 16 and 17 the flow rate could not be measured (the upper limit of the used flowmeter range is at about 0.6 g/s). Nevertheless the acoustic spectrum could be evaluated above this range and its example at such

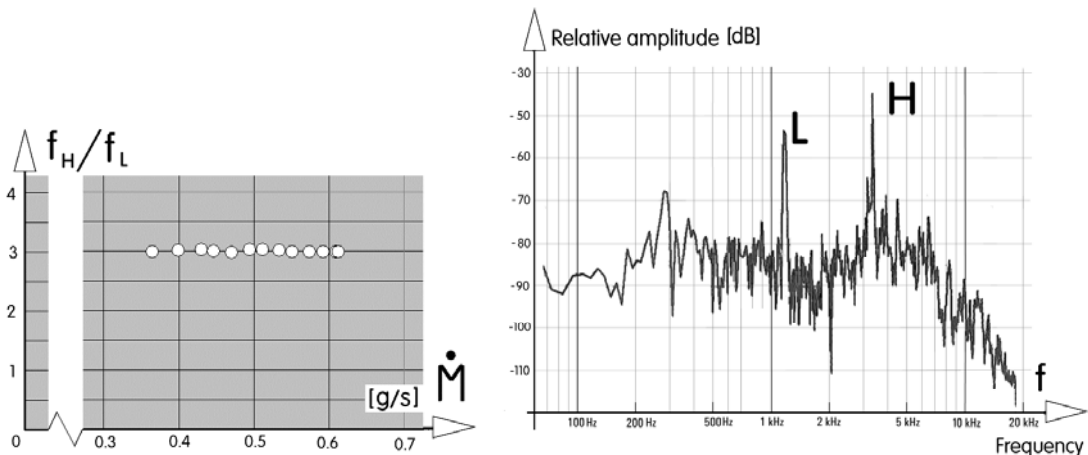


Fig. 18 (Left) The ratio of the frequency of the two peaks in the spectra (Fig. 17) at various air flow rates. The factor 3.0 between the two frequencies is obvious.

Fig. 19 (Right) Acoustic spectrum measured at a very high air flow rate 3.7 g/s (beyond the range of the flowmeter that was used to obtain data in Figs. 16 and 22). The peak corresponding to the third harmonic of the basic switching frequency is here as well — but typically for the high flow rates, it is here dominating the spectrum.

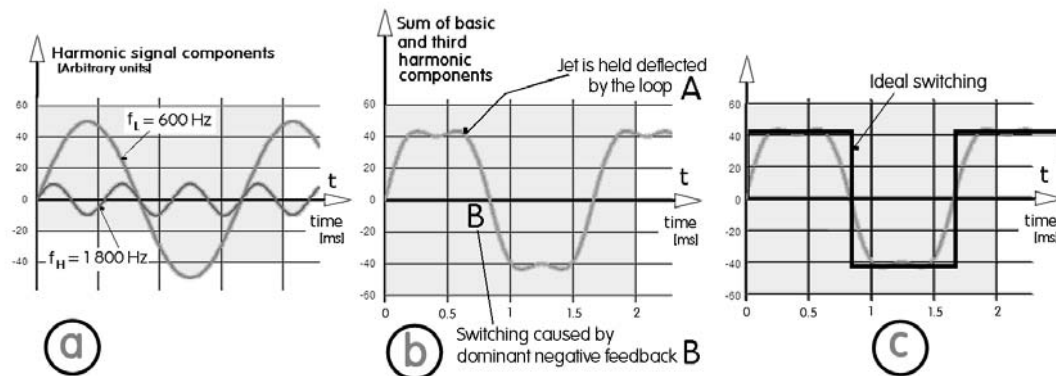


Fig. 20 Explanation of the meaning and importance of the third harmonic. At left, in diagram (a), are plotted two sinusoidal oscillations: one at frequency $f_L = 600$ Hz, the other one (with smaller amplitude) at $f_H = 1800$ Hz. In the central diagram (b) these two components are superposed. As shown at right-hand diagram (c), the result of the summation is an approximation to a switching between two regimes.

larger flows is presented in Fig. 19. There is again the lower frequency f_L and its third harmonic f_H . The marked difference in comparison with Fig. 17 is the dominance of the third harmonic H at the very high flow rates. In the aerator, the two driving frequencies have the same effect as if they were generated by two different sources. The strong agitation at the high frequency, commensurable with natural oscillation of very small microbubbles, can produce them – either by releasing them from the aerator exits or by fragmentation in what otherwise would be larger bubbles.

The question of why there is the third harmonic in the spectrum of the oscillation is easy to answer with the help of Fig. 20. In its left-hand part (a) are shown two sinusoidal functions with frequencies corresponding to the two spectral organised components $f_L = 600$ Hz and $f_H = 1800$ Hz. as if generated from two separate sources, an L source and an H source, the high-frequency source H in this case of lower intensity. If these two components are summed, as is done in the central part (b) of Fig. 20, the result roughly approximates a switching between two constant values. It is a well-known fact that Fourier analysis of rectangular pulses, such as shown by the heavy line in the right-hand part (c) of Fig. 20 contains solely odd harmonics of the switching frequency f

$$f + 3f + 5f + 7f + 9f \dots$$

In fluidic devices higher harmonics tend to be filtered out, so that a relative good approximation to the rectangular wave train passing through a fluidic device is

$$f + 3f + 5f$$

In the present case, the acoustic signal may be approximately

$$f_L + 3f_L,$$

- or, because of $f_H = 3f_L$

$$f_L + f_H$$

It is assumed that the presence of the H source plays the decisive role in the size of generated microbubbles. While the basic L oscillation, at $f_L = 600$ Hz, is seen in Fig. 15 to generate bubbles of diameter 0.8 mm - just passing the criterion of what is called a microbubble (< 1 mm), but not likely to be very much different from behaviour of larger bubbles, the microbubbles generated by the third harmonic at $f_H = 1800$ are really small, of diameter less than 0.4 mm.

The first author's idea of the character of the air flows in the cavities, as was presented above in Fig. 13, may be now compared with the wavetrain shapes in Fig. 2-0. Initially after the jet is switched to one side of the splitter, the positive vortical feedback A keeps the jet deflected (without this action it would be difficult to explain why the jet remains deflected (and the output signal is at nearly constant level in Fig. 20 b) in the absence of the attachment walls and the Coanda effect of jet attachment. Later the substantial part of the air flow deflected by the sharp nose at the inlet into the oscillator output channel and thereafter having run along the walls of the feedback cavity, forms the vortical loop B. This causes the amplifier to switch to the mirror-image position, where the same sequence of phenomena takes place.

5. Additional investigations: small aspect ratio and smaller feedback cavities

One of the key problems in the development of the integrated microbubble generation unit is the problem of matching the oscillator with the aerator. In a simplistic way this problem may be characterised as oscillator needing large flow rates (for Reynolds number indicating a turbulent flow regime) while aerator can handle only rather small flows. Balancing these requests is easier if the integral

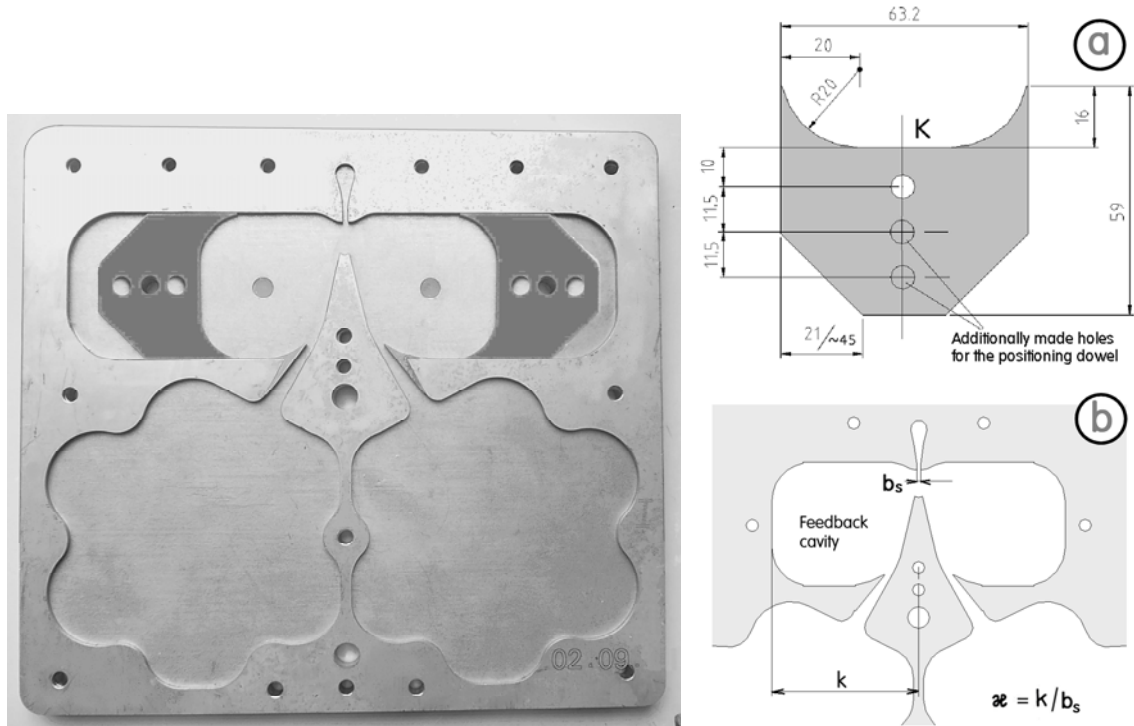


Fig. 21 (Left) Photograph of the investigated unit in the with single, 2 mm thin main plate and two inserts (dark) placed into the feedback cavities to decrease their size. **Fig. 21a (Right, top)** Workshop drawing of the inserts. **Fig. 21b (Right, bottom)** Definition of the relative distance α used for characterisation of the feedback cavity size.

unit is designed with large aerator while the oscillator is small. Since aerator properties from the fluidic point of view are more complex than originally expected, the matching procedure contained too many unknowns. To cater for possible problems, the oscillator was made in a form with an allowance for simple variation of properties: it was laser cut in stacked stainless steel plates so that the nozzle aspect ratio could be varied by varying the number of the plates in the stack. The results of the aspect ratio change were not easy to predict. Earlier experience tended to indicate, since the aerodynamic processes with small number of plates are inevitably hampered by increased importance of fluid friction on the top and bottom cover plates, that with the small number of the main plates the behaviour was likely to deteriorate. It was believed that the consequent damping of the jet switching motion — and of the vortical motions inside the feedback cavities — could reach the scale at which the oscillation would no be possible at all.

Quite surprisingly, the experience gained from experimental investigations discussed in this paper disproved these expectations. On the contrary, with the nozzle exit aspect ratio as small as the seemingly rather hopeless $h / b_s = 1$, i.e. with just the single main plate, the integral unit was found not only operating properly, but in fact offering an excellent performance. On the basis of absolute values of the supplied air mass flow rate the performance was in fact better than with the larger aspect ratios. One of the factors of high importance, the minimum flow magnitude at which the oscillator still generates oscillation as the flow is decreased, was found in these experiments as follows:

- with the original aspect ratio $h / b_s = 3$ the magnitude was 0.18 g/s (Fig. 16)
- with the decreased aspect ratio $h / b_s = 1$ the magnitude was 0.045 g/s (Fig. 22)

The other performance parameter of utmost interest in the present context is the magnitude of the frequency of generated oscillation. How effective is the action at the natural frequency of microbubbles has yet to be investigated experimentally, nevertheless acting at resonance seems to be quite certainly a correct approach so that the quest after high-frequency oscillator is reasonable. The results discussed above, with frequency of basic jet switching at about 600 Hz were quite encouraging – and the presence of the third harmonic 1800 Hz especially promising.

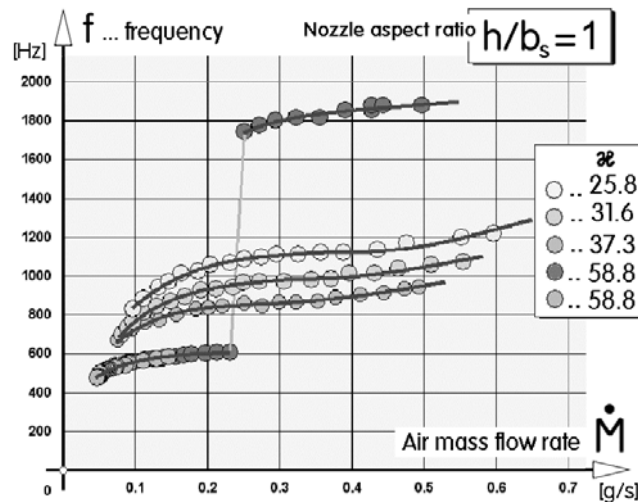


Fig. 22 Dependence of oscillation frequency on air mass flow rate found experimentally with different relative distances ζ of the single main plate configuration if Fig. 21. Values near to the desirable kHz are achievable, but of particular importance (in a manner somewhat analogous to the three plates configuration, Fig. 16) is the high frequency of the third harmonic dominating the oscillation with the empty feedback cavities ($\zeta = 58.8$).

Whatever feedback mechanism is present - the vortical motions suggested in Fig. 13 may be correct, but some acoustic resonance in the cavities is also a possibility - decreasing the size of the cavities on both sides of the splitter in the oscillator must lead to higher frequencies. In the vortical flow the length of the feedback path will be shorter – and the resonator theory will also profit from the shorter resonant wavelength.

The idea was tested in the configuration presented in Fig. 21, with the adjustable insert in the cavities – and with the small aspect ratio (a single main plate in the stack). The results of the experiment are presented in Fig. 22. Obviously frequencies above the 1 kHz are achievable in the basic jet switching mode – and in a similar manner to Fig. 16 there is again at higher flow rates a presence of strong third harmonic.

6. Conclusions

The new version of the microbubble generator contains in a single submersible body – a stack of stainless steel plates - two integral stainless-steel woven textile aerators and a simultaneously made oscillator. Originally, the oscillator corresponded to the classical layout of Coanda effect bistable amplifier with two feedback channels, made by laser cutting in the same plate as the oscillator cavities. The task was to find the configuration with small air flow rate and high oscillation frequency. These requirements were fulfilled in the unusual version with feedback cavities resulted by removal of isolated "islands" – parts of the plate that fell out during the cutting of the feedback channels and originally were inserted back into their position. The tests concentrated on identifying the consequence of varying aspect ratio by removal of some of the stacked plates and also on changing the available size of the feedback cavities. The absence of Coanda-effect attachment walls did not cause any troubles – apparently due to the positive feedback effect of the bi-cuspid splitter. In some tested configurations the oscillation was dominated by

third harmonic of the basic jet-switching frequency. The resultant high-frequency component is considered a particular opportunity for generating very small microbubbles.

Acknowledgments

Gratefully acknowledged is support obtained by research grant Nr. 13-23046S from GAČR, by grant TA02020795 provided by TAČR, and institutional support RVO:61388998.

References

- [1] Liger-Belair G., et al.: *On the velocity of expanding spherical gas bubbles rising in line in supersaturated hydroalcoholic solutions: Application to bubble trains in carbonated beverages*, Langmuir, Vol. 16, p. 1889, 2000
- [2] Hepworth N.J., et al.: *Characterizing gas bubble dispersions in beer*, Food and Bioproducts Processing, Vol. 79, p.13, 2001
- [3] Tesař V.: *Interesting properties of microbubbles*, Proc. of 27th symposium on Anemometry, Litice, Czech Republic, 4-5 June 2013
- [4] Tesař V.: *Microbubble generation by fluidics. Part I: Bubble formation mechanism*, Proc. of Colloquium 'Fluid Dynamics 2012', Prague, October 2012
- [5] Engel T.P.: *Diffusor and methods of using the same*, European Patent Application EP 0135822 A2, Filed Aug. 1984
- [6] Zimmerman W. B., Tesař V., Butler S., Bandulasena H.: *Microbubble generation*, Recent Patents in Engineering, Vol. 2: p.1, 2008
- [7] Zimmerman W.B., Tesař V.: *Bubble generation for aeration and other purposes*, British Patent GB20060021561, Filed Oct. 2006,
- [8] Tesař V.: *Microbubble generation by fluidics. Part II Development of the oscillator*, Proc. of Colloquium 'Fluid Dynamics 2012', Prague, October 2012
- [9] Tesař V., Hung C.-H., Zimmerman W. B.: *No-moving-part hybrid-synthetic jet actuator*, Sensors and Actuators A, Vol. 125, p. 159, 2006
- [10] Tesař V.: *A mosaic of experiences and results from development of high-performance bistable flow-control elements*, Proc. of Conf. 'Process Control by Power Fluidics', Sheffield, 1975
- [11] Tesař V.: *"Optimum loading of fluidic unvented jet-deflection valves"*, Proc. of 2nd Conf. Control of fluid systems, ISBN 80-7100-452-9, p. 25, Žilina, Slovakia, November 1997
- [12] Tesař V.: *"Fluidic Control of Reactor Flow – Pressure Drop Matching"*, Chemical Engineering Research and Design, Vol. 87, p. 817, 2009
- [13] Zimmerman W. B., Hewakandamby B. N., Tesař V., Bandulasena H.C.H., Omotowa O. A.: *On the design and simulation of an airlift loop bioreactor with microbubble generation by fluidic oscillation*. Food Bioprod. Process, Vol. 87:p. 215, 2009
- [14] Zimmerman W.B., Zandi M., Bandulasena H.C.H., Tesař V., Gilmour D.J., Ying K.: *Design of an airlift bioreactor and pilot scale studies with fluidic oscillator induced microbubbles for growth of a microalgae Dunaliella Salina*, Applied Energy, Vol. 88, p. 335, 2011
- [15] Tesař V., Šonský J.: *"Near-exit coalescence – a so far unknown limit to microbubble smallness"*, Proc. of Conf. 'Topical problems of Fluid Mechanics', p. 73, Praha 2013
- [16] Tesař V., Zhong S., Fayaz R.: *"New fluidic oscillator concept for flow separation control"*, AIAA Journal, Vol. 51, p. 397, 2013
- [17] Tesař V., Peszynski K.: *"Strangely behaving fluidic oscillator"*, European Physics Journal Web of Conferences, Vol. 45, paper number 01074, 2013
- [18] Tesař V., Peszynski K.: *"Water oxygenation by fluidic microbubble generator"*, Proc of Conf EFM 2013 Experimental Fluid Mechanics, Kutná Hora, 2013